Compton scattering study of the electron momentum density in Sr_2RuO_4

N. Hiraoka, A. Deb, M. Itou, and Y. Sakurai*
Japan Synchrotron Radiation Research Institute (JASRI), SPring-8, 1-1-1 Kouto, Sayo, Mikazuki, Hyogo, 679-5198, Japan

Z. Q. Mao and Y. Maeno
Department of Physics, Kyoto University, Kyoto, 606-8502, Japan
and CREST, Japan Science and Technology Corporation, Kawaguchi, Saitama, 332-0012, Japan
(Received 27 March 2002; revised manuscript received 23 October 2002; published 26 March 2003)

The electron momentum density of the unconventional superconductor Sr_2RuO_4 has been studied using the high-resolution Compton scattering technique. Compton profiles have been measured along the [100], [110], and [210] directions, and compared with theoretical profiles calculated using the full potential linearized augmented plane wave method within the local density approximation. The calculated and measured electron momentum distributions, as obtained by the Compton profiles, are in good agreement with respect to their overall shapes and anisotropies in the Compton profiles. Theoretical analyses have shown that the amplitude of the anisotropies is dominated by the filled bands which possess Ru $4d$ and O $2p$ bonding characters in the RuO_2 planes.

DOI: 10.1103/PhysRevB.67.094511 PACS number(s): 74.78.Fk, 78.70.Ck, 71.18.+y, 71.15.Ap

I. INTRODUCTION

The layered perovskite oxide Sr_2RuO_4 has attracted considerable attention since the discovery of superconductivity in this compound.[1] Although the value of T_c is about 1.5 K, Sr_2RuO_4 has been intensively studied since it is isostructural with the $(La,Sr)_2CuO_4$ high-T_c superconductors, and it possesses partially filled d bands that are strongly hybridized with O p orbitals in the same way as the cuprates. In spite of these similarities, various studies have revealed essential differences between the ruthenate and the cuprates. In Sr_2RuO_4, superconductivity occurs in a normal state that is well described as a Landau-Fermi liquid,[2,3] in contrast to the anomalous normal state of the cuprates. A series of studies[4,5] provided lines of evidence that spin-triplet Cooper pairs with p-wave symmetry are formed in the superconducting state of Sr_2RuO_4,[6] while the high-T_c cuprate superconductors have a spin-singlet pairing with d-wave symmetry. These differences are conceivably attributed to the nature of their valence bands.

A central issue to understand the differences is the electron correlation effects which may modify the Fermi surface (FS) geometry and the energy dispersion that are predicted by the band theory. Regarding the cuprates, the local spin density approximation fails to describe the magnetism of undoped systems properly, mostly due to the presence of strong electron correlations. A theoretical study of $YBa_2Cu_3O_7$ has shown that the on-site electron correlation certainly modifies the geometry of the FS and the energy dispersion which are obtained by the band theory.[7] Turning to ruthenates, the band theory predicts the correct magnetic behaviors and phases in $(Ca,Sr)RuO_3$ and Sr_2YRuO_6 and the insulating character of Sr_2YRuO_6.[8] Moreover, the local density approximation (LDA) calculations for Sr_2RuO_4 (Refs. 9 and 10) have provided a shape of the FS which is quite consistent with the de Haas–van Alphen (dHvA) experiments.[2,11–13] The multiband quasiparticle calculations have presented that the geometry of the LDA FS is not changed by the inclusion of Hubbard-type electron correlation.[14] However, early angle-resolved photoemission spectroscopy (ARPES) experiments[15–17] have presented a different FS geometry. The difference comes from the detection by ARPES of a dispersive feature at the M point which is interpreted as an extended van Hove singularity pushed down just below the Fermi energy by strong electron correlations. Recently, ARPES has been carried out once again, and the results reported are very sensitive to the experimental condition, e.g., the incident x-ray energy and temperature of the sample cleaving; an analysis with special care is required to reproduce the LDA FS.[18] The different FS observed in previous ARPES studies is ascribable to the lattice reconstruction on the surface, found in scanning tunneling microscopy.[19] Therefore, the validity of a LDA-based theory on predicting the electronic structure and relevant quantities of Sr_2RuO_4 is still inconclusive in connection with the influence of electron correlations. The present issue is to settle this situation by obtaining information about the electronic structure of Sr_2RuO_4 with a complementary technique.

The aim of the present study is to measure the electron momentum density distributions in Sr_2RuO_4 using the Compton scattering technique. This paper shows that LDA-based band theory predicts the experimental results well with respect to their overall shapes and anisotropies in the Compton profiles. A theoretical analysis shows that the LDA result reproduces the low momentum part of the density distributions better than that artificially obtained with an upward shift of the Fermi energy. It is also presented that the LDA properly predicts the filled bands without having recourse to the strong electron correlation effects.

In a Compton scattering experiment, one measures the so-called Compton profile,[20,21]

$$J(p_z) = \int \int n(\mathbf{p}) dp_x dp_y , \tag{1}$$

where p_z is the momentum component along the scattering vector. The Compton profile $J(p_z)$ is given as a one-

dimensional projection of the electron momentum density, $n(\mathbf{p})$, onto the p_z axis. In an independent-particle model, the momentum density is given by

$$n(\mathbf{p}) = (2\pi)^{-3} \sum_{\nu,\mathbf{k},\mathbf{G}}^{occ.} \delta(\mathbf{k}+\mathbf{G}-\mathbf{p}) \left| \int \psi_{\mathbf{k},\nu}(\mathbf{r}) e^{i\mathbf{p}\cdot\mathbf{r}} d\mathbf{r} \right|^2, \tag{2}$$

where $\psi_{\mathbf{k},\nu}(\mathbf{r})$ denotes the electron wavefunction in state $\mathbf{k}$ and band ν, and $\mathbf{G}$'s are reciprocal lattice vectors.[22] The summation in Eq. (2) extends over all occupied states. The low momentum part of the Compton profile reflects the geometry of the Fermi surface in the underlying three-dimensional momentum density $n(\mathbf{p})$. This technique also probes the phenomenon of bonding through a modulated structure in the Compton profile.[23] Unlike ARPES, Compton scattering is very bulk sensitive, and unlike dHvA and angular correlation of positron annihilation radiation (ACAR) measurements it is insensitive to defects and impurities in a sample. These notable features provide complementary information about the electronic structure of Sr_2RuO_4.

II. EXPERIMENT

A single crystal of Sr_2RuO_4 was grown by a floating zone method. It has a nearly rectangular shape with a size of $3 \times 5 \times 15$ mm^3. It was confirmed to exhibit a superconducting transition at $T_c = 1.43$ K. The Compton profile measurements were carried out at room temperature at the BL08W beamline of SPring-8. The reader is referred to Hiraoka *et al.*[24] for details of the Compton spectrometer. The incident x-ray energy was 115.5 keV, and the scattering angle was 165°. The overall momentum resolution was 0.14 atomic units (a.u.). The Compton profiles were measured along the [100], [110], and [210] directions. The obtained Compton profiles were corrected for the background x rays, photoabsorption in the sample, the scattering cross section, detection efficiency of the spectrometer, and double scattering. The double-Compton-scattering events were simulated via a Monte Carlo program;[25] the integrated intensity of the double-scattering events was found to be 15.2 % of the sum of the single- and double-scattering events. The background x rays were correctly subtracted since the position sensitive detector employed in the spectrometer had an energy resolution to discriminate between signals and backgrounds.[24,26]

III. COMPUTATIONS

The crystal structure of Sr_2RuO_4 is of K_2NiF_4 type, with the $I4/mmm$ space group.[27] The atomic coordinates are given by Sr(0,0,z(Sr)), Ru(0,0,0.5), O(I)(0,0.5,0), and O(II)(0,0,z(O)). The lattice constants and parameters are $a = 3.8603$ Å, $c = 12.729$ Å, $z(\mathrm{Sr}) = 0.14684$, and $z(\mathrm{O}) = 0.3381$.

The self-consistent calculations were carried out using the full potential linearized augmented plane wave (LAPW) method.[28] With regard to the exchange correlation potential, the form of Perdew and Wang was employed.[29] The valence band states were treated in a scalar relativistic approximation, while the core states were calculated relativistically. The valence (Sr $5s$, Ru $4d$ and $5s$, O $2s$ and $2p$) and semicore (Sr $4s$ and $4p$, Ru $4s$ and $4p$) states were treated in the same energy window by using local orbitals as an extension to the LAPW basis set. Muffin-tin sphere radii were set to 2.20, 1.95, 1.65, and 1.85 a.u. for Sr, Ru, in-plane O(I), and apical O(II) atoms, respectively. The cutoff $RK_{max} = 8.5$ was used, providing well converged basis sets and leading to about 500 basis functions per primitive cell. Inside the atomic spheres the charge density and the potential were expanded in crystal harmonics up to $l = 6$. The radial basis functions of each LAPW were calculated up to $l = 10$ and the nonspherical potential contribution to the Hamiltonian matrix had an upper limit of $l = 4$. The Brillouin zone integration was performed using the modified tetrahedron method[30] with 240 $\mathbf{k}$ points in the irreducible wedge of the Brillouin zone, and the reciprocal lattice vectors $\mathbf{G}$'s were extended up to 11.5 a.u.

In order to obtain the Compton profiles the momentum density $n(\mathbf{p})$ was calculated on a mesh containing 240×2109 $\mathbf{p}$ points, where 240 denoted the number of $\mathbf{k}$ points in the irreducible wedge of the Brillouin zone, and 2109 the number of $\mathbf{p}$ points obtained from each $\mathbf{k}$ point by adding reciprocal lattice vectors. The two-dimensional integrations involved in the evaluation of the Compton profiles [see Eq. (1)] were carried out by utilizing the tetrahedron method of Lehmann and Taut.[31] Finally the theoretical Compton profiles along the [100], [110], and [210] directions were computed up to $p_z = 10.0$ a.u. with a momentum mesh of 0.02 a.u. The geometry of the Fermi surface obtained by the present calculation is in good accord with those of the previous reports,[9,10] where the electron sheets (β and γ) are centered at the Γ point and the hole sheet (α) is at the X point.

IV. RESULTS AND DISCUSSION

Figure 1 shows the measured (open circles) and the theoretical (solid lines) Compton profiles (CPs) of the valence electrons along the [100], [110], and [210] directions, where the calculated CPs are convoluted with an experimental resolution function. The raw data, the calculated core profile, and the double scattering contribution for the [100] directional CP are presented in inset (a) of Fig. 1. The experimental valence CPs have been obtained by subtracting the calculated core CPs (Ref. 32) from the measured profiles. The height of the experimental CPs are reproduced well by the theoretical calculations. This fact is in contrast to the previous findings in simple metals and alloys, where the heights of LDA-based theoretical CPs were higher than that of experiments[34–40] For comparison, the Lam-Platzman correction is displayed in inset (b) of Fig. 1. Although slight discrepancies are observed in a region between $p_z = 1$ and 4 a.u., there is a good accord between the experiment and theory with respect to the overall shapes of the CPs.

Figure 2 presents the low momentum parts of the experimental CP (open circles) along the [100] direction, together with that of the LDA-based calculation (solid line). The calculated profile is convoluted by the experimental resolution

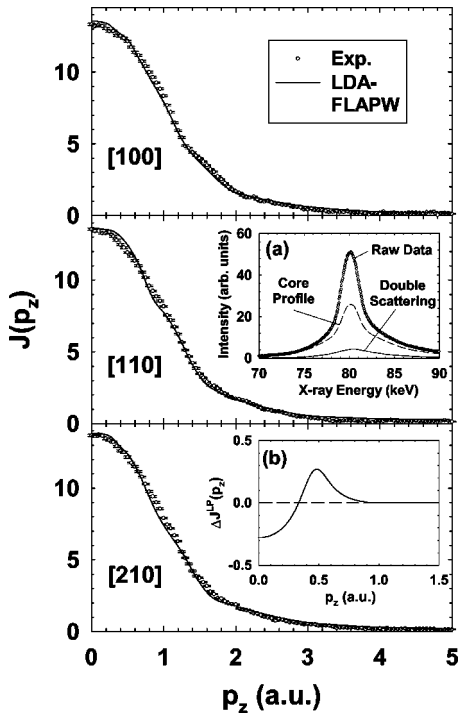

FIG. 1. Experimental Compton profiles (CPs) (open circles) and calculated CPs (solid lines) for Sr_2RuO_4. The calculated CPs are convoluted with the experimental resolution function. Inset (a) shows the raw data, the core profile, and the double scattering contribution for the experimental CP along the [100] direction. Inset (b) is the Lam and Platzman correction.

function. In order to highlight the sharp structures related to the geometry of the FS, the profile without the resolution convolution (dash-dotted line) is also shown in Fig. 2. In order to clarify the origin of the fine structures in the theoretical profile, bandwise profiles for the partially filled

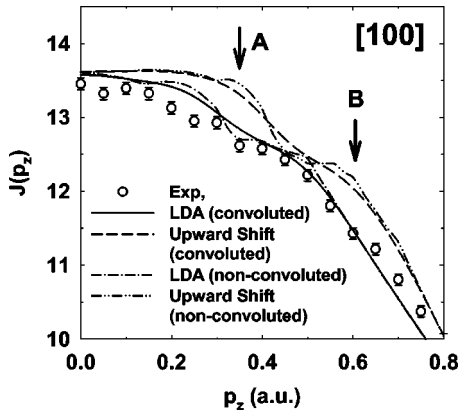

FIG. 2. Experimental Compton profile (CP) (open circles) and calculated Compton profiles in the low momentum region. The solid line shows the result of the LDA-based calculation and the dashed line is that obtained by the artificial upward shift of the Fermi energy by 0.06 eV, where both calculated profiles are convoluted by the experimental resolution function. The calculated profiles without the resolution convolution are shown to highlight sharp structures related to the geometry of the Fermi surface.

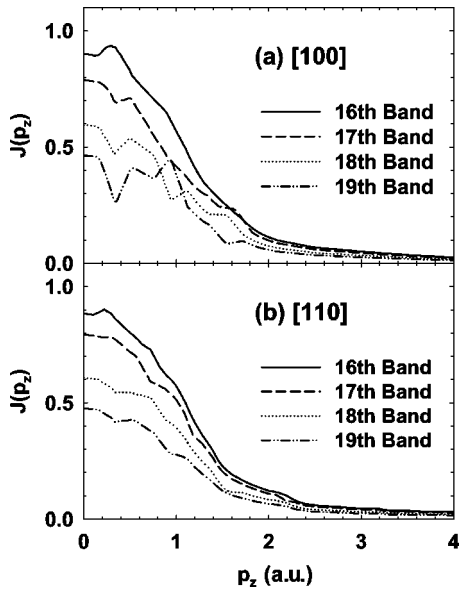

FIG. 3. Theoretical bandwise profiles of the partially filled (17th–19th) and highest filled (16th) bands: (a) [100] directional profiles, (b) [110] directional profiles.

(17th–19th) and highest filled (16th) bands are presented for the [100] direction in Fig. 3(a). The theoretical FS is composed of two electron sheets (β and γ) centered at the Γ point and a hole sheet at the X point. The projection of the bodies of the β and γ sheets and their higher components ($\mathbf{G}\neq 0$) onto the [100] direction makes a dip at 0.35 a.u. in the 19th and 18th band profiles. The hole pockets of the α sheet also

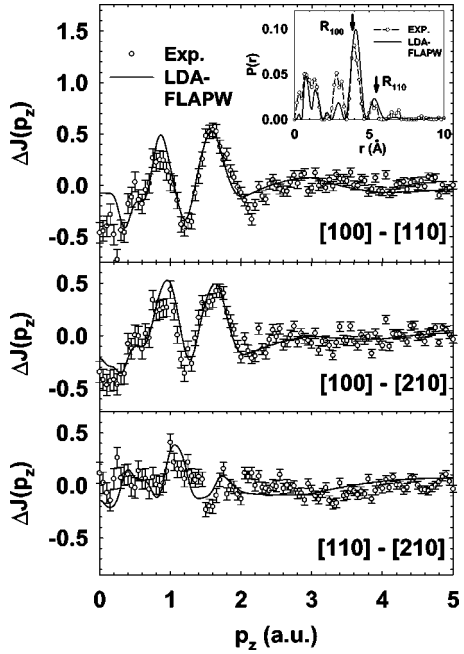

FIG. 4. Experimental (open circles) and theoretical (solid lines) anisotropy profiles. The power spectrum of the [100]-[110] anisotropy profile is shown in the inset, where R_{100} and R_{110} indicate the shortest distances between Ru atoms along the [100] and [110] directions.

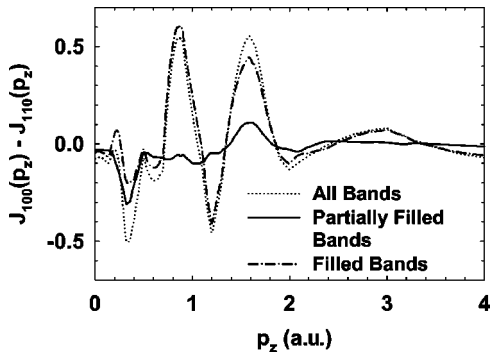

FIG. 5. Calculated anisotropies ([100]-[110]) for all (1st–19th), partially filled (17th–19th), and filled (1st–16th) bands. The filled bands dominate the anisotropies between the [100] and [110] directional Compton profiles.

produce a dip at 0.35 a.u. in the 17th band profile. On the other hand, the 16th band profile presents a peak at 0.30 a.u. The interplay between the dip due to the FS geometry and the peak due to the occupied state makes the structure around 0.35 a.u. In the bandwise profiles along the [110] direction, projection of γ and β gives a shallow dip at 0.35 a.u. in the 18th and 19th bands, while that of α makes a small peak in the 17th band [see Fig. 3(b)]. This cancellation leads to no detectable FS signature in the CP along the [110] direction.

In order to examine how the change of the FS geometry affects these low momentum parts, we have artificially shifted the Fermi level by 0.06 eV upward, and computed the CPs again. The idea of making adjustments to the LDA FS by shifting the Fermi energy (i.e., a rigid band shift) has been employed for an interpretation of ARPES spectra.[15–17] The upward shift makes the γ electron sheet disappears at the M point, leading to a FS with one electron sheet centered at the Γ point and two hole sheets at the X point. As shown in Fig. 2, the present upward shift brings additional amounts of momentum density in the CPs (indicated by A and B), implying that the upwardly shifted FS is unacceptable in Sr_2RuO_4.

Figure 4 displays the anisotropies in the CPs of Fig. 1. The bandwise anisotropy profiles ([100]–[110]) are presented in Fig. 5. As is evident in Fig. 5, the anisotropies come from the filled bands except for the structure at $p_z = 0.35$ a.u. The filled bands are mainly the bonding states of the Ru $4d$ and in-plane O $2p$ orbitals, and the nonbonding states of O $2p$.[9] Since the nonbonding states do not cause any modulation in the CP, anisotropic fine structures are assigned to the bonding states. As seen in the inset of Fig. 4, the power spectrum $P(r)$ of the anisotropy profile ([110]–[110]) shows peaks which could be identified with the interatomic distances, where R_{100} and R_{110} indicate the shortest Ru-Ru distances along the [100] and [110] directions. In the independent particle model, $P(r)$ can be written as

$$P(r) = |B_{110}(r) - B_{100}(r)|^2, \tag{3}$$

and

$$B_{hkl}(r) = \sum_j \int \psi_j(\mathbf{s}) \psi_j^*(\mathbf{s}+\mathbf{r}) d\mathbf{s}, \tag{4}$$

where $\psi_j(\mathbf{r})$'s are the position space wavefunctions and $\mathbf{r}$ is taken along the $[hkl]$ direction.[23] Several other peaks observed in the experimental and calculated $P(r)$'s could be understood as the behavior of the total autocorrelation function of the wave functions. Till now, several experiments have reported that the presence of bonding gives rise to a periodic oscillation and an angular dependence in the momentum density.[41–44] According to simple models,[23] the amplitude of modulated structures depends on the overlap integral of atomic wavefunctions at different sites. Therefore, the oscillatory behavior in the CP and thus the anisotropies serve as a critical test for the theoretical predictions for the bonding states. As is obvious in Fig. 4, the amplitude of the experimental anisotropies is in good agreement with that of the LDA computations. This indicates that the present calculation gives the correct wave functions in the filled Ru $4d$ bands that are hybridized with O $2p$ orbitals. This fact is in contrast to the case of the cuprate $YBa_2Cu_3O_{7-x}$ where the LDA calculation predicted a 40% larger amplitude in the anisotropy profile than the experiment.[42,45] In the cuprate, it is likely that the LDA-based theory does not properly describe the bonding states in the CuO_2 planes because of strongly correlated electrons. Theoretically, it was reported that on-site correlation modifies the single-particle band structure even at the high binding energy region around 12 eV in $YBa_2Cu_3O_7$.[7]

V. SUMMARY

We have measured the Compton profiles (CPs) of Sr_2RuO_4 along the [100], [110], and [210] directions at an x-ray energy of 115.5 keV with a momentum resolution of 0.14 a.u. In parallel with the experiments, full potential LAPW calculations have been carried out within the LDA-based band theory framework. Comparisons between the experiment and theory show a good level of accord in the overall shapes of the CPs, the height of CPs, and the anisotropies of a pair of CPs. An artificial rigid band shift, where the Fermi energy is shifted upward by 0.06 eV, has worsened the agreement between the experiments and calculations. An examination of the anisotropy profiles has also shown that the theory well predicts the wave functions of Ru $4d$ and O $2p$ bonding states in the RuO_2 planes. Finally, the Compton scattering provides information on the electronic structure of complex materials, complementary to ARPES, dHvA, and ACAR measurements.

ACKNOWLEDGMENTS

We acknowledge N. Sakai and A. Koizumi for valuable discussions. We also thank A. Shukla for useful information about the Compton profiles of $Y(Pr)Ba_2Cu_3O_{7-x}$. This work was supported by the SPring-8 Research Promotion Scheme under the auspices of the Japan Science and Technology Corporation and performed with the approval of JASRI (Proposal No. 2001B0497-ND-np).

*FAX: +81-719-58-0830. Email address: sakurai@spring8.or.jp

[1] Y. Maeno, H. Hashimoto, K. Yoshida, S. Nishizaki, T. Fujita, J. G. Bednorz, and F. Lichtenberg, Nature (London) **372**, 532 (1994).
[2] A. P. Mackenzie, S. R. Julian, A. J., Diver, G. J. McMullan, M. Ray, G. G. Lonzarich, Y. Maeno, S. Nishizaki, and T. Fujita, Phys. Rev. Lett. **76**, 3786 (1996).
[3] Y. Maeno, K. Yoshida, H. Hashimoto, S. Nishizaki, S. Ikeda, M. Nohara, T. Fujita, A. P. Mackenzie, N. E. Hussey, J. G. Bednorz, and F. Lichtenberg, J. Phys. Soc. Jpn. **66**, 1405 (1997).
[4] K. Ishida, H. Mukada, Y. Kitaoka, K. Asayama, Z. Q. Mao, Y. Mori, and Y. Maeno, Nature (London) **396**, 658 (1998).
[5] G. M. Luke, Y. Fudamoto, K. M. Kojima, M. I. Larkin, J. Merrin, B. Machumi, Y. J. Uemura, Y. Maeno, Z. Q. Mao, Y. Mori, H. Nakamura, and M. Sigrist, Nature (London) **394**, 558 (1998).
[6] T. M. Rice and M. Sigrist, J. Phys.: Condens. Matter **7**, L453 (1995).
[7] S. Monastra, F. Manghi, and C. Ambrosch-Draxl, Phys. Rev. B **64**, 020507 (2001).
[8] I. I. Mazin and D. J. Singh, Phys. Rev. B **56**, 2556 (1997).
[9] T. Oguchi, Phys. Rev. B **51**, 1385 (1995).
[10] D. J. Singh, Phys. Rev. B **52**, 1358 (1995).
[11] A. P. Mackenzie, S. Ikeda, Y. Maeno, T. Fujita, S. R. Julian, and G. G. Lonzarich, J. Phys. Soc. Jpn. **67**, 385 (1998).
[12] Y. Yoshida, R. Settai, Y. Onuki, H. Takei, K. Betsuyakum, and H. Harima, J. Phys. Soc. Jpn. **67**, 1677 (1998).
[13] C. Bergemann, S. R. Julian, A. P. Mackenzie, S. NishiZaki, and Y. Maeno, Phys. Rev. Lett. **84**, 2662 (2000).
[14] A. Liebsch and A. Lichtenstein, Phys. Rev. Lett. **84**, 1591 (2000).
[15] T. Yokoya, A. Chainani, T. Takahashi, H. Ding, J. C. Campuzano, H. Katayama-Yoshida, M. Kasai, and Y. Tokura, Phys. Rev. B **54**, 13 311 (1996).
[16] T. Yokoya, A. Chainani, T. Takahashi, H. Katayama-Yoshida, M. Kasai, and Y. Tokura, Phys. Rev. Lett. **76**, 3009 (1996).
[17] D. H. Lu, M. Schmidt, T. R. Cummins, S. Schuppler, F. Lichtenberg, and J. G. Bednorz, Phys. Rev. Lett. **76**, 4845 (1996).
[18] A. Damascelli, D. H. Lu, K. M. Shen, N. P. Armitage, F. Ronning, D. L. Feng, C. Kim, Z.-X. Shen, T. Kimura, Y. Yokoya, Z. Q. Mao, and Y. Maeno, Phys. Rev. Lett. **85**, 5194 (2000).
[19] R. Matzdorf, Z. Fang, Ismail, Jiandi Zhang, T. Kimura, Y. Tokura, K. Terakura, and E. W. Plummer, Science **289**, 746 (2000).
[20] See, e.g., *Compton Scattering*, edited by B. Williams (McGraw-Hill, London, 1977).
[21] N. Shiotani, Jpn. J. Appl. Phys. **38-1**, 18 (1999).
[22] A. Bansil, Z. Naturforsch., A: Phys. Sci. **48**, 165 (1993).
[23] W. Weyrich, P. Pattison, and B. G. Williams, Chem. Phys. **41**, 271 (1979).
[24] N. Hiraoka, M. Itou, T. Ohata, M. Mizumaki, Y. Sakurai, and N. Sakai, J. Synchrotron Radiat. **8**, 26 (2001).
[25] N. Sakai, J. Phys. Soc. Jpn. **56**, 2477 (1987).
[26] Y. Sakurai, N. Hiraoka, M. Itou, M. Mizumaki, T. Ohata, A. Deb, H. Toyokawa, M. Suzuki, and N. Sakai, J. Phys. Chem. Solids **62**, 2099 (2001).
[27] L. Walz and F. Lichtenberg, Acta Crystallogr., Sect. C: Cryst. Struct. Commun. **49**, 1268 (1993).
[28] P. Blaha, K. Schwarz, P. Sorantin, and S. B. Tricky, Comput. Phys. Commun. **59**, 399 (1990).
[29] J. P. Perdew and Y. Wang, Phys. Rev. B **45**, 13 244 (1992).
[30] P. E. Blöchl, O. Jepsen, and O. K. Andersen, Phys. Rev. B **49**, 16 223 (1994).
[31] G. Lehmann and M. Taut, Phys. Status Solidi B **54**, 469 (1974).
[32] The calculated core profile is in excellent agreement with that obtained from the free atom Hartree-Fock calculation by Biggs *et al.* (Ref. 33).
[33] F. Biggs, L. B. Mendelsohn, and J. B. Mann, At. Data Nucl. Data Tables **16**, 201 (1975).
[34] M. J. Cooper, Rep. Prog. Phys. **48**, 415 (1985).
[35] N. Shiotani, Y. Tanaka, Y. Sakurai, N. Sakai, M. Ito, F. Itoh, T. Iwazumi,and H. Kawata, J. Phys. Soc. Jpn. **62**, 239 (1993).
[36] Y. Sakurai, Y. Tanaka, A. Bansil, S. Kaprzyk, A. T. Stewart, Y. Nagashima, T. Hyodo, S. Nanao, H. Kawata, and N. Shiotani, Phys. Rev. Lett. **74**, 2252 (1995).
[37] M. Itou, Y. Sakurai, T. Ohata, A. Bansil, S. Kaprzyk, Y. Tanaka, H. Kawata, and N. Shiotani, J. Phys. Chem. Solids **59**, 99 (1997).
[38] Y. Sakurai, S. Kaprzyk, A. Bansil, Y. Tanaka, G. Stutz, H. Kawata, and N. Shiotani, J. Phys. Chem. Solids **60**, 905 (1999).
[39] Y. Kubo, Y. Sakurai, and N. Shiotani, J. Phys.: Condens. Matter **11**, 1683 (1999).
[40] T. Ohata, M. Itou, I. Matsumoto, Y. Sakurai, H. Kawata, N. Shiotani, S. Kaprzyk, P. E. Mijnarends, and A. Bansil, Phys. Rev. B **62**, 16 528 (2000).
[41] E. D. Isaacs, A. Shukla, P. M. Platzman, D. R. Hamann, B. Barbiellini, and C. A. Tulk, Phys. Rev. Lett. **82**, 600 (1999).
[42] A. Shukla, B. Barbiellini, A. Erb, A. Manuel, T. Buslaps, V. Honkimäki, and P. Suortti, Phys. Rev. B **59**, 12 127 (1999).
[43] A. Shukla, E. D. Isaacs, D. R. Hamann, and P. M. Platzman, Phys. Rev. B **64**, 052101 (2001).
[44] A. Koizumi, S. Miyaki, Y. Kakutani, H. Koizumi, N. Hiraoka, K. Makoshi, N. Sakai, K. Hirota, and Y. Murakami, Phys. Rev. Lett. **86**, 5589 (2001).
[45] A. Shukla, B. Barbiellini, E. Erb, A. Manuel, T. Buslaps, V. Honkimäki, and P. Suortti, J. Phys. Chem. Solids **61**, 357 (2000).